ACS APPLIED MATERIALS & INTERFACES

Research Article

www.acsami.org

Novel TiO_2/PEGDA Hybrid Hydrogel Prepared in Situ on Tumor Cells for Effective Photodynamic Therapy

Hui Zhang,[†] Ronghua Shi,[‡] Anjian Xie,[†] Juchuan Li,*[,§] Long Chen,[†] Ping Chen,[†] Shikuo Li,[†] Fangzhi Huang,[†] and Yuhua Shen*[,†]

[†]School of Chemistry and Chemical Engineering, Anhui University, Hefei 230039, P. R. China

[§]Department of Chemical and Materials Engineering, University of Kentucky, Lexington, Kentucky 40506, United States

[‡]School of Life and Science, University of Science and Technology of China, Hefei 230027, P. R. China

Supporting Information

ABSTRACT: A novel inorganic/organic hybrid hydrogel system containing titanium dioxide (TiO_2)/poly(ethylene glycol) double acrylates (PEGDA) was prepared by in situ photopolymerization on tumor cells for photodynamic therapy (PDT). TiO_2 nanorods with diameter of ~5 nm and length of ~25 nm in this system presented dual functions, as effective photosensitizers for PDT and initiators for causing the in situ formation of hydrogel, under near-infrared (NIR) irradiation. The hybrid hydrogel retained the TiO_2 around tumor cell to form a drug-loaded hydrogel shell. This resulted in a high concentration of singlet oxygen ($^1O_2$) under NIR irradiation, which induced apoptosis of tumor cell. Also, the hydrogel could reduce the side effects by preventing TiO_2 from migrating to normal tissue. Furthermore, the TiO_2 nanorods in this hydrogel shell were photochemically recyclable and could be reused in regular treatment. The outcomes of this study provide a new way to exploit multifunction of inorganic semiconductor nanomaterials for a variety of biomedical applications.

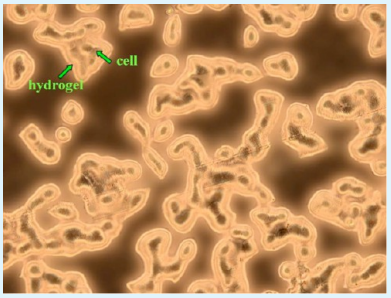

KEYWORDS: *TiO_2/PEGDA, hybrid hydrogel shell, photodynamic therapy, tumor cell*

INTRODUCTION

Photodynamic therapy (PDT) is an emerging treatment for a variety of cancers.[1] Compared with conventional cancer therapies, such as surgery, radiotherapy, and chemotherapy, the localized high-dose PDT strategy results in beneficial high therapeutic efficacy, and reduced side effects for healthy tissues.[2] The most commonly used photosensitizers in PDT are porphyrin based molecules. These organic or organometallic dyes are, however, prone to photoinduced degradation and enzymatic degradation, which brings concerns to PDT treatments and reduces the efficiency of the generation of singlet oxygen.[3]

Inorganic nanoparticles have recently become widely used in biomedical applications, including drug delivery, imaging diagnosis, and disease therapeutics.[4] TiO_2 nanoparticles are perhaps the most widely used semiconductor. They have been applied in the phototherapy of malignant cells, and are potential PDT photosensitizing agent, because of their high stability and irradiation-induced phototoxicity. However, drawbacks for the clinical use of TiO_2 include insufficient selectivity and low efficiency, which arise from the lack of tumor-specific accumulation of TiO_2. Thus, TiO_2 nanoparticles must be modified with biomolecules that specifically bind cancer cells, which is a complex and costly process.[5] It is of great importance to find an appropriate method to reduce the flow of TiO_2 nanoparticles or even concentrate the TiO_2 nanoparticles to construct a localized PDT system in the field of medical nanotechnology.

Hydrogel could encapsulate bioactive substances by simply mixing them in precursor liquids and then transforming the liquid solution into cross-linked hydrogel network. The bioactive substances are confined in cross-linked network of hydrogel and localized at the defect sites, which are important properties in tissue engineering and drug delivery.[6] Poly(ethylene glycol) double acrylate (PEGDA) hydrogel has been widely investigated, because the PEG segment is nonimmunogenic, nontoxic, and hydrophilic.[7] PEGDA hydrogel prepared by photopolymerization have advantages over those prepared by conventional chemical cross-linking, because of the minimally invasive delivery.[8] Many photoinitiators such as IRGACURE 2959 are activated by ultraviolet light, and become harmful to the human body. Thus, using near-infrared (NIR) wavelengths (>600 nm) is usually required.[9]Furthermore, using inorganic/organic hydrogel matrix to immobilize semiconductor photosensitizers on tumor cells to maximize their PDT efficiency under NIR irradiation has not been reported.

In this study, a TiO_2/PEGDA hydrogel was prepared on tumor cells for PDT, through in situ photopolymerization. TiO_2 nanorods prepared by a sol–gel method were used as

Received: June 29, 2013
Accepted: November 18, 2013
Published: November 18, 2013

both photosensitizer for antitumor and photoinitiator for the polymerization of PEGDA. As illustrated in Scheme 1, the precursor was incubated with the cells in lesion site, and then rapidly converted into the hydrogel on the cell surface, after NIR laser irradiation (λ = 650 nm). Cancer cells are simultaneously killed by singlet oxygen ($^1O_2$) released from TiO_2 and oxygen. The hydrogel shell prevents TiO_2 from migrating throughout the body, so that the anticancer activities could be enhanced and normal cells are less damaged. Moreover, because TiO_2 is a recyclable material in photochemistry, this hydrogel system has characteristics of simple preparation process, low cost, high curative effect, and low dosage, and may be used for regular treatment in PDT.

Scheme 1. Schematic Illustration of the TiO_2/PEGDA Hydrogel Formed on Tumor Cells by Photopolymerization

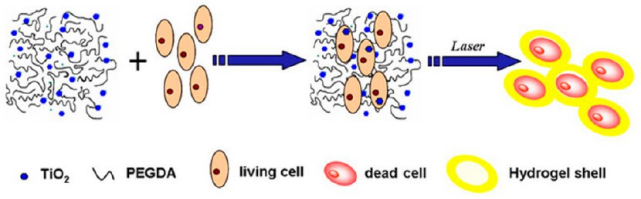

EXPERIMENTAL SECTION

Materials. PEGDA ($M_n \approx 575$ g mol^{-1}), potassium dihydrogen phosphate (KH_2PO_4), disodium hydrogen phosphate (Na_2HPO_4), sodium chloride (NaCl), potassium chloride (KCl), and dimethylsulfoxide (DMSO) were obtained from Aladdin Reagent Database Inc. (Shanghai, P. R. China). 3-(4,5-Dimethyl-2-thiazolyl)-2−5-diphenyl-2*H*-tetrazolium bromide (MTT), Hoechst 33342, and propidium iodide (PI) were obtained from Sangon Company (Shanghai, P. R. China). 1,3-Diphenylisobenzofuran (DPBF) was purchased from Acros Organics (Geel, Belgium). Fluorescein isothiocyanate-dextran (FITC-dex, M_w = 70 kDa) was purchased from Sigma-Aldrich (Germany). All reagents were of analytical grade and were used without further purification. Double distilled water was used throughout.

Synthesis of TiO_2 Nanorods. TiO_2 nanorods were synthesized by the hydrolysis of tetrabutyl titanate. In brief, 3.5 mL of tetrabutyl titanate was added to a solution containing 47 mL of water and 8 mL of acetic acid. After magnetic stirring for 1.5 h, the transparent sol was collected for further experiments. The photopolymerization of the PEGDA precursor was initiated by TiO_2 with NIR irradiation. In a typical experiment, 0.02 mg of TiO_2 sol was added to 0.25 mL of PEGDA in a quartz cuvette. The cuvette was located 2 cm from the light source in a darkroom. The mixture was irradiated by a 200-mW 650-nm laser diode for 5 min, where it gradually changed to a semisolid hydrogel. Experiments were performed with TiO_2 sol:PEGDA volume ratios of 2%, 5%, 8%, 10%, and 12%, to understand the influence of TiO_2 concentration on PEGDA photopolymerization. A commercial TiO_2 initiator was also tested using the same method.

Transmission electron microscopy (TEM) images of TiO_2 nanorods were obtained using a JEM 2100 instrument. The phase structure and purity of the TiO_2 were examined by X-ray diffraction (XRD), using a MAP18XAHF diffractometer with Cu K_α radiation (λ = 1.54 Å). The $^1O_2$ generated from TiO_2/PEGDA under NIR irradiation was determined by monitoring the decrease of the absorption at 410 nm from the decomposition of DPBF in ethanol UV−vis spectra. ROS determined by the decomposition of DPBF correlated to the decay of the absorption at 410 nm (Supporting Information Figure S2).The irradiation wavelength used to excite the sensitizer was 650 nm, and absorption spectra were measured by a UV-1800 spectrophotometer (Shimadzu Corp., Japan). For quenching $^1O_2$, mechanistic studies were carried out using scavenging OH (DMSO, 4 μL), prior to the addition of the complexes. Fourier transform infrared spectroscopy (FT-IR) measurements were recorded using a NEXUS-870 instrument. Fluorescence images were recorded on a DMI3000B inverted fluorescence microscope (Leica, Germany).

Cytotoxicity Assay and Uptake Studies. HeLa cells were maintained in RPMI 1640 (Gibco, U.S.A.) medium supplemented with 10% fetal calf serum (Sigma, USA) at 37 °C, with 5% CO_2 in a 95% humidity atmosphere. Cell viability was determined by a MTT assay. HeLa cells were seeded into 96-well plates, and incubated in the cell culture growth medium for 24 h. Hydrogel precursors of specific concentrations were added to the plates, and incubated for a further 24 h. The cells were then transferred to a fresh growth medium. One of the plates was kept in the dark, while the others were exposed to light. The plates were then incubated for 6 h (37 °C, 5% CO_2), and MTT reagent was then added to each well. After incubation for 4 h, a solubilization solution (10% sodium dodecyl sulfate in 0.01 M HCl) was added to each well. Following centrifugation, the absorbance of the medium was recorded using a microplate reader at 490 nm. All experiments were repeated eight times to ensure reproducibility.

For fluorescence microscope imaging, HeLa cells were incubated for 24 h in chamber slides, at a density of 5×10^3 cells/cm^2 of hydrogel precursor. Cells were then stained with Hoechst 33342 (10 μg mL^{-1}) and PI (10 μg mL^{-1}) for 15 min in the dark before imaging. Dual fluorescently stained cells were washed and observed under an inverted fluorescence microscope. Experiments were repeated three times.

To quantify the dextran uptake, HeLa cells (4.0×10^4/well) were cultured in a 24-well microplate at 37 °C for 48 h in medium. After complete adhesion, the cells were washed twice with serum-free medium, and then incubated in serum-free medium for 1 h. Cells were then treated with fresh serum-free medium containing FITC-dextran (1 mg mL^{-1}), in the presence of hydrogel precursor at 37 °C for 1 h, washed by PBS buffer, and observed under a fluorescence microscope using excitation wavelengths of 488 nm.

Apoptosis was also determined by assessment of TUNEL staining assay. HeLa cells were treated with and without precursor for 48 h, and then fixed in 10% neutral buffered formaldehyde for 10 min. Slides were rinsed with PBS, and incubated with blocking solution (3% H_2O_2 in methanol) for 10 min at room temperature. Slides were rinsed with PBS, and incubated in permeabilization solution (0.1% TritonX-100 in 0.1% sodium citrate) for 2 min on ice. Slides were rinsed with PBS, and TUNEL reaction mixture was added to the samples. Slides were incubated for 60 min at 37 °C, in a humidified atmosphere in the dark. Fluorescence microscopy was used to identify apoptotic cell nuclei, as indicated by their distinct green color change.

RESULTS AND DISCUSSION

Semiconductor photocatalysis is a surface process, so the photochemical activity of small TiO_2 particles is higher than that of larger particles. Figure 1a shows a TEM image of the TiO_2 colloidal particles, which exhibit rod shapes with diameters of ~5 nm and lengths of ~25 nm. The XRD pattern of the TiO_2 nanorods (Figure 1b) exhibits six major reflection peaks at 2θ of 25.2°, 38.5°, 48.0°, 55.0°, 62.6°, and 70.3°, which can be well indexed to the (101), (112), (200), (211), (204), and (220) planes of anatase TiO_2 (JCPDS Card No. 21−1272), respectively.

The optical properties of the TiO_2 nanorods were measured by ultraviolet−visible diffuse reflectance spectroscopy (UV−vis DRS). Strong absorption in the visible region is observed in the UV−vis DRS spectrum, shown in inset in Figure 1c. The optical band gap energy E_g for a semiconductor can be estimated by

$$(\alpha h\nu)^n = A(h\nu - E_g) \quad (1)$$

where α, h, and ν are the absorption coefficient, Planck's constant, and frequency, respectively. A is a constant of the

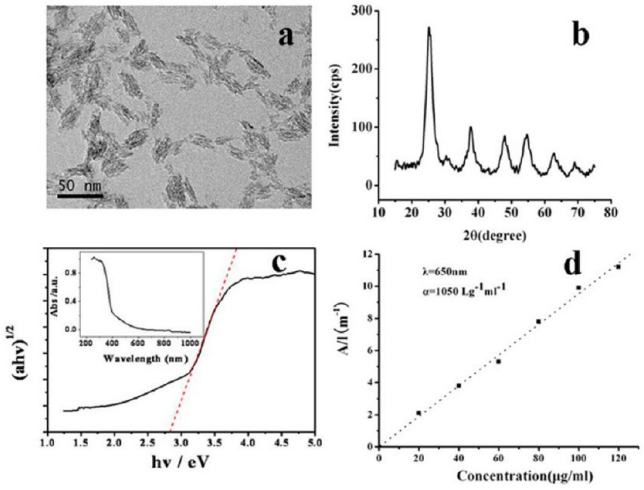

Figure 1. (a) TEM image, (b) XRD pattern, and (c) $(\alpha h\nu)^2$ versus $h\nu$ plot and (inset) UV–vis DRS spectrum of prepared TiO_2 nanorods. (d) Optical absorbance (λ = 660 nm) divided by cell length, as a function of TiO_2 nanorod concentration.

material, and n is either 2 for direct interband transition or 1/2 for indirect interband transition. Figure 1c shows the $(\alpha h\nu)^2$ versus $h\nu$ curve for the TiO_2 nanorods. The band gap of the sample is about 2.8 eV by extrapolation of the above equation, while bulk TiO_2 with large size (Supporting Information Figure S1a) has a higher bandgap (3.4 eV, Supporting Information Figure S1b). The photochemistry of TiO_2 is affected by its size, shape, crystalline structure, and surface structure. The results suggest that the TiO_2 nanorods should possess favorable photochemistry properties, when irradiated under visible light.[10] According to a previous report,[11] anatase and rutile TiO_2 can also be activated in visible and NIR region attributed to the donor–acceptor recombination, and trapped electrons with free holes under weak excitation condition.[11] The peak absorbance at 650 nm divided by cell length is plotted versus concentration in Figure 1d,[12] showing Lambert–Beer behavior with an average absorption coefficient (α_{650}) of 1050 L g^{-1} m^{-1}. Thus, NIR irradiation was employed and compared with visible light irradiation, for determining the formation conditions of TiO_2/PEGDA hydrogel.

The effect of visible light and NIR irradiation on hydrogel formation with different TiO_2 concentration is summarized in Table 1 and Figure 2. When the ratio of TiO_2 to PEGDA is 2% (v/v), no hydrogel is formed by either visible light or NIR irradiation for 5 min (Figure 2a). When the TiO_2/PEGDA ratio is 5% (v/v), a homogeneous semisolid hydrogel is produced (Figure 2b). While visible light is more effective than NIR irradiation for the photopolymerization of PEGDA, NIR is a more suitable light source for laser acupuncture and moxibustion, because it can penetrate biotic tissues without heating effects. It is concluded that the optimum TiO_2/PEGDA ratio for the NIR photopolymerization of PEGDA is 10% (v/v), and this ratio is used in the following experiments. The TiO_2 particle size also plays an important role in the hydrogel formation. Commercially available TiO_2 has an average particle size of 500 nm (Supporting Information Figure S1a) and band gap of 3.4 eV (Supporting Information Figure S1b). Such large TiO_2 particles are found difficult to initiate PEGDA polymerization under any doses (Figure 2c). These results indicate that the TiO_2 nanorods with a small size and proper aspect ratio are effective NIR photoinitiator. Figure 2d shows a TEM image of the hydrogel, in which TiO_2 nanorods can be seen embedded in the hydrogel. Arrows 1 and 2 indicate TiO_2 nanorods and the hydrogel, respectively.

Table 1. Effect of Visible and NIR Irradiation on Hydrogel Formation for Different TiO_2/PEGDA Ratios

	hydrogel-forming time (min)	
volume ratio of TiO_2 sol to PEGDA (%)	visible	NIR
5	2.5	10
8	2	8
10	2	5
12	3	10

The FT-IR spectrum of the hydrogel is shown in curve 1 of Figure 2e. The 1725 cm^{-1} peak is assigned to the C═O stretching vibration. The peak at 1110 cm^{-1} due to the asymmetric stretching vibration of −C−O−C groups in TiO_2/PEGDA hydrogel is weakened compared with precursor (curve 2). The results indicate that titanium ions coordinate with the C═O groups of PEGDA, contribute to the combination of photosensitizer with hydrogel, and maintain the high concentration of photosensitizer to improve the treatment effect. Peaks at 1640, 990, and 810 cm^{-1} attributing to the C═C bonds of the acrylates in the PEGDA macromers disappeared after NIR irradiation, suggesting that most macromers have been polymerized.

To evaluate the capability of TiO_2 in generating reactive oxygen species (ROS) (e.g, $^1O_2$ and $\dot{O}H$) in the PEGDA precursor liquid under NIR irradiation, DPBF was used as a detector. ROS determined by the decomposition of DPBF correlated to the decay of the absorption at 410 nm (Supporting Information Figure S2). Figure 3a plots the ROS output of freshly prepared TiO_2/PEGDA as a function of NIR irradiation time. About 9.1 × 10^{-8} mol of DPBF was completely decomposed within 5 min, reflecting a very high ROS yield. The ability of TiO_2 nanorods to regenerate ROS under NIR irradiation was also investigated, by monitoring the absorbance at 410 nm after 3, 5, and 7 days. TiO_2/PEGDA had a significant ROS output of 90.4% (Figure 3b) after 3 days. The ROS output decreasesd slightly to 88% after 5 days (Figure 3c), and was still relatively high (74%) after 7 days (Figure 3d). This fact implies that the TiO_2/PEGDA has a high stability and reusability, and is suitable as a photosensitizer in intermittent PDT treatment.

To test if $^1O_2$ is the main cause of DPBF degradation, photocleavage experiments were carried out in the presence of an $\dot{O}H$ scavenger, such as DMSO. Supporting Information Figure S3 shows that high activities are observed in the presence of DMSO, suggesting that $^1O_2$ is the reactive species responsible for DPBF degradation.

The stability of the hydrogel on the surface of cells was further investigated. Figures 4a and b show optical microscopy images of bare HeLa cells, and HeLa cells treated by the TiO_2/PEGDA precursor under NIR irradiation, respectively. Figure 4b shows that a homogeneous continuous hydrogel shell (indicated by arrow 1) forms on the cells (arrow 2) after photopolymerization. The average shell thickness is ~5 μm. Multiple interactions including hydrogen bonding and van der Waals forces exist between PEG chains, sugar chains, proteins, and phosphatidylcholine on the cell surface.[13−16] These interactions assist the formation of the TiO_2/PEGDA hydrogel

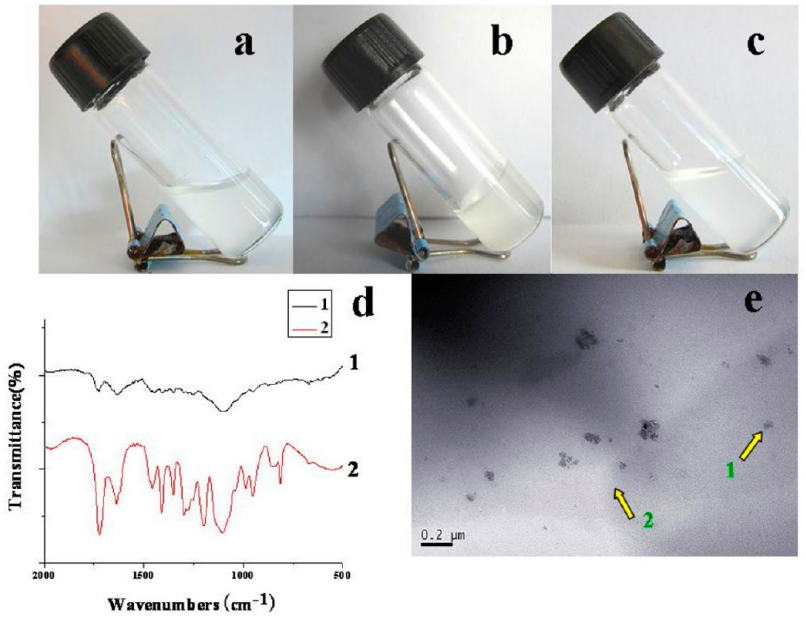

Figure 2. Photograph of TiO_2/PEGDA precursor prepared at the volume ratios of (a) 2% and (b) 10% (v/v), after NIR irradiation for 5 min, and (c) commercial TiO_2 after NIR irradiation for 5 min, (d) FT-IR spectra of (1) TiO_2/PEGDA hydrogel and (2) TiO_2/PEGDA precursor. (e) TEM image of TiO_2/PEGDA hydrogel showing TiO_2 nanorods (arrow 1) and hydrogel (arrow 2).

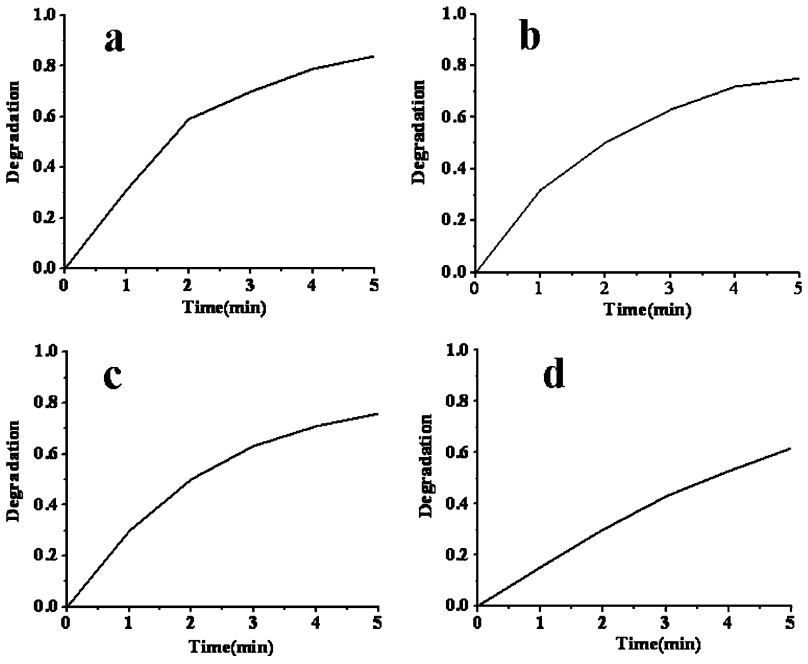

Figure 3. Photodecomposition of DPBF by ROS, upon the NIR irradiation of the TiO_2/PEGDA precursor with DMSO every two days, (a) 1, (b) 3, (c) 5, and (d) 7 days.

shell on tumor cells. The shell is thought to trap photosensitizers on the tumor cells, and prevent their migration to normal tissue. The shell also retains a high photosensitizer concentration on lesions, which enhances antitumor activity under irradiation.

To verify the cytotoxicity of TiO_2/PEGDA, we used MTT assay to examine the viability of HeLa cells coated by the TiO_2/PEGDA hydrogel. Cells were incubated with different TiO_2/PEGDA concentrations for 24 h. The biocompatibility of TiO_2/PEGDA is shown in Figure 5. The cell survival rate trends downward with increasing TiO_2/PEGDA concentration. The cell survival rate is 82.2% and 67.5% in the absence of irradiation, for TiO_2/PEGDA precursor concentrations of 0.03 and 0.3 M, respectively. Cell viability is still 56% at a TiO_2/PEGDA concentration of 3 M. The concentration-dependent results indicate that TiO_2/PEGDA has low cytotoxicity, and that it is biocompatible. Under NIR irradiation, the viability of cells treated by TiO_2/PEGDA is 87.1%, 35.4%, and 12.0%, for TiO_2/PEGDA precursor concentrations of 0.03, 0.3, and 3 M, respectively. With this in mind, TiO_2 nanorods within the hydrogel are effective in the PDT treatment of tumor cells.

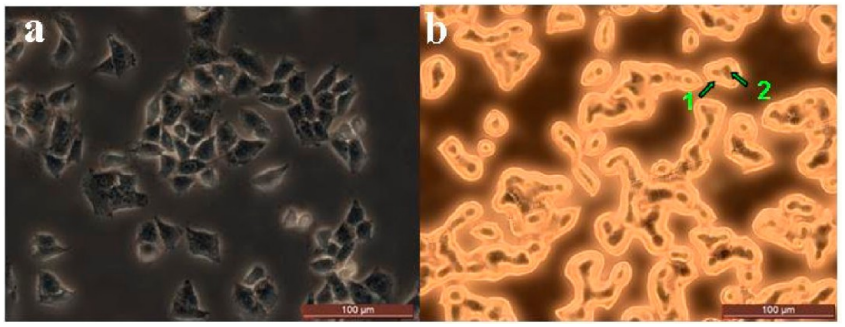

Figure 4. Microscopy images of (a) bare HeLa cells and (b) HeLa cells coated with hydrogel shells. Arrows 1 and 2 indicate a hydrogel shell and HeLa cell, respectively.

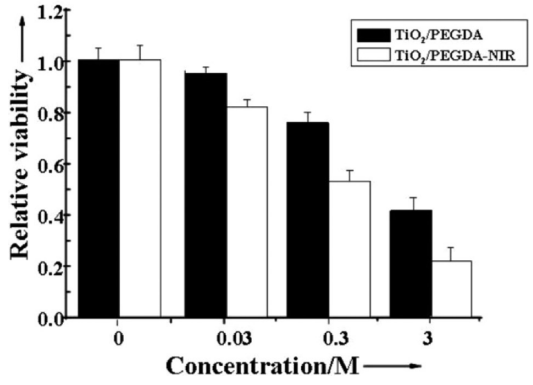

Figure 5. Viability of HeLa cells with different TiO_2/PEGDA precursor concentrations in the presence and absence of NIR irradiation.

The cellular uptake and antitumor effect of the TiO_2/PEGDA precursor were investigated by fluorescence microscope with PI/Hoechst 33342 double staining (Figure 6). After culturing for 6 h without TiO_2/PEGDA, cell death is not observed under NIR irradiation. Almost all HeLa cells remain healthy, without their nuclei appearing red (Figure 6a). Figure 6b shows cells incubated with the TiO_2/PEGDA precursor without NIR irradiation. Few cells appear stained by PI (red fluorescence), indicating the low toxicity of TiO_2/PEGDA, in agreement with the MTT results. When the same HeLa cells are cultured with the TiO_2/PEGDA precursor and then subjected to NIR irradiation for 5 min, most cells dead with their nuclei turning red (Figure 6c). HeLa cells are effectively killed by $^1O_2$ generated from TiO_2 nanorods and oxygen during polymerization. Most cells lose their membrane integrity, as evident by the enlarged view shown in the inset in Figure 6c, which promotes the transport of photosensitizer to cell interiors, and strengthens its penetrability of the cell membrane. The change of the membrane permeability could be due to PEG segment of PEGDA, which induces cell fusion.[17] These findings suggest that PEGDA can act as a transmembrane carrier to increase cell internalization and decrease the photosensitizer efflux. This facilitates the photosensitizer accumulation within cell.

The couptake of TiO_2/PEGDA in HeLa cells was studied by FITC-dextran labeling and fluorescence microscopy. Compared with the control group (Figure 7a), the green fluorescence (Figure 7b) of FITC-dextran labeled TiO_2/PEGDA indicates its internalization within cells.

Morphological changes of the cells were studied to confirm apoptosis. The evaluation of normal or apoptotic cells depends

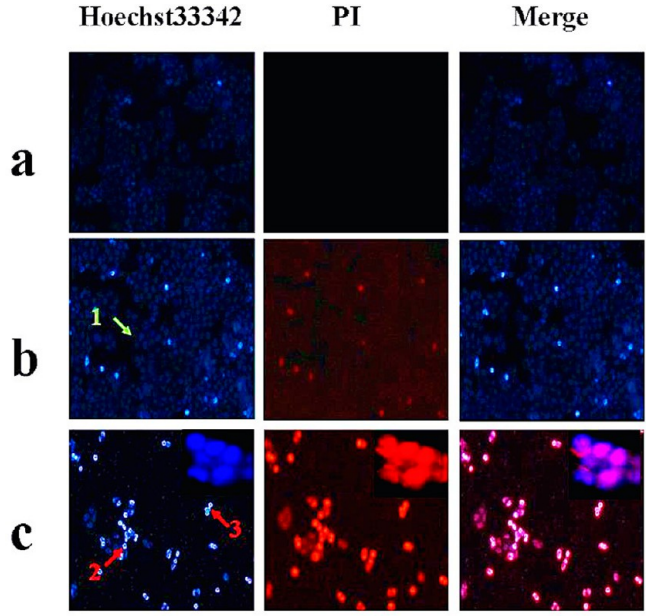

Figure 6. In vitro phototoxicity tests of (a) bare cells under NIR irradiation, and cells treated with the TiO_2/PEGDA precursor before (b) and after (c) NIR irradiation. Enlarged views of cells are shown inset in the top right of (c). Arrow 1 indicates a normal cell with a smooth nucleus. Arrows 2 and 3 indicate cells with apoptotic nuclear condensation and fragmentation.

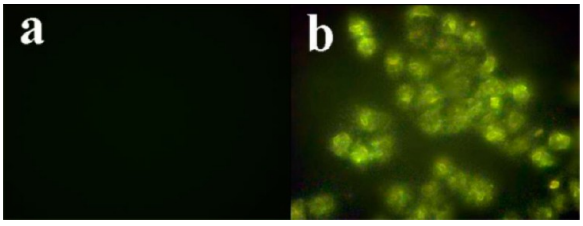

Figure 7. Fluorescence microscopy images showing the localization of (a) FITC-dextran with HeLa cells and (b) FITC-dextran labeled TiO_2/PEGDA with HeLa cells.

on morphological characterization. The normal cell with smooth nuclei is indicated by arrow 1 in Figure 6b. Cells with apoptotic nuclear condensation and fragmentation are indicated by red arrows 2 and 3 in Figure 6c, respectively. These findings imply that TiO_2/PEGDA kills cancer cells under NIR irradiation by inducing apoptosis, rather than by necrosis.

To further determine whether the hydrogel precursor induces cell apoptosis, a cell apoptosis assay was performed

using TUNEL as an apoptosis marker (green color). There are hardly any apoptotic cells to be detected before the NIR irradiation of TiO_2/PEGDA, as shown in Figure 8a. After irradiation for 5 min, apoptosis is apparent (Figure 8b). This result suggests that TiO_2/PEGDA might promote apoptosis of HeLa cells by means of NIR irradiation.

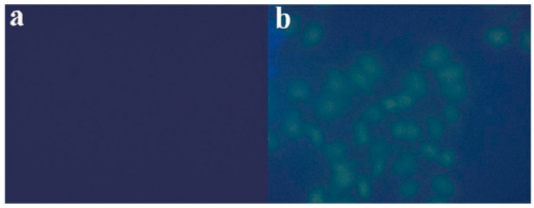

Figure 8. TUNEL staining of HeLa cells treated by (a) TiO_2/PEGDA and (b) TiO_2/PEGDA-NIR.

CONCLUSIONS

A TiO_2/PEGDA hydrogel was prepared on tumor cells, and exhibited high stability and phototoxicity. The TiO_2 nanorods also presented high photoinitiating ability, and upon NIR irradiation rapidly transformed the precursor into a hydrogel. TiO_2 nanorods were an excellent photosensitizer, generating $^1O_2$ which resulted in tumor cell apoptosis under NIR irradiation. The hydrogel prevented TiO_2 nanorods from migrating to normal tissue, thus avoiding side effects and maintaining an effective TiO_2 concentration at the tumor cells. This approach could be expanded to other antineoplastic agents for antitumor applications.

ASSOCIATED CONTENT

Supporting Information

SEM images, UV−vis DRS spectra, and $(\alpha h\nu)^2$ verses $h\nu$ plots of commercially available titania,and UV−vis detection of DPBF decomposition correlated to the absorbance decay at 410 nm. This material is available free of charge via the Internet at http://pubs.acs.org.

AUTHOR INFORMATION

Corresponding Authors

*E-mail: jlin@g.uky.edu.
*E-mail: s_yuhua@163.com.

Notes

The authors declare no competing financial interest.

ACKNOWLEDGMENTS

This work is supported by the National Natural Science Foundation of China (91022032, 51202001, 21171001 and 21173001) and Anhui Province Key Laboratory of Environment- friendly Polymer Materials.

REFERENCES

(1) Yamaguchi, S.; Kobayashi, H. T.; Narita, K.; Kanehira, S.; Sonezaki, N.; Kudo, Y.; Kubota, S.; Terasaka; Houkin, K. *Ultrason. Sonochem* **2011**, *18*, 1197−1204.
(2) Harada, Y. K.; Ogawa, Y.; Irie, H.; Endo, L. B.; Feril, T., Jr; Uemura; Tachibana, K. *J. Controlled Release* **2011**, *149*, 190−195.
(3) Zhang, H.; Chen, B.; Jiang, H.; Wang, C.; Wang, H.; Wang, X. *Biomaterials* **2011**, *32*, 1906−1914.
(4) Lagopati, N.; Kitsiou, P. V.; Kontos, I.; Venieratos, P.; Otsopoulou, E.; Kontos, K A. G.; Dionysiou; Pispas, D. D.; Tsilibary, S. E. C.; Falaras, P. *J. Photochem. Photobiol., A* **2010**, *214*, 215−223.
(5) Qin, Y.; Sun, L.; Li, X.; Cao, Q.; Wang, H.; Tang, X.; Ye, L. *J. Mater. Chem.* **2011**, *21*, 18003−18010.
(6) Rioux, D.; Laferrière, M.; Douplik, A.; Shah, D.; Lilge, L.; Kabashin, A. V.; Meunier, M. M. *J .Biomed. Opt.* **2009**, *14*, 021010−021010.
(7) Hah, H. J.; Kim, G.; Lee, Y.-E.; Orringer, K. D. A.; Sagher, O.; Philbert, M. A.; Kopelman, R. *Macromol. Biosci.* **2011**, *11*, 90−99.
(8) Rozhkova, E. A.; Ulasov, I.; Lai, B. N.; Dimitrijevic, M.; Lesniak, M. S.; Rajh, T. *Nano Lett.* **2009**, *9*, 3337−3342.
(9) Ding, H. H.; Yu, Y.; Dong, R.; Tian, G.; Huang, D. A.; Boothman, B. D.; Sumer; Gao, J. *J. Control. Releas.* **2011**, *156*, 276−280.
(10) Dong, P.; Wang, Y.; Guo, L.; Liu, B.; Xin, S.; Zhang, J. *Nanoscale* **2012**, *15*, 4641−4649.
(11) Wang, X. Z.; Feng, J.; Shi, G.; Jia, S.; Shen, J.; Zhou; Li, C. *Phys. Chem. Chem. Phys.* **2010**, *12*, 7083−7090.
(12) Hernandez, Y.; Nicolosi, V.; Lotya, M.; Blighe, F. M.; Sun, Z. Y.; De, S.; McGovern, I. T.; Holland, B.; Byrne, M.; Gun'Ko, Y. K. *Nat. Nanotechnol.* **2008**, *3*, 563−568.
(13) Teramura, Y.; Kaneda, Y.; Totani, T.; Iwata, H. *Biomaterials* **2008**, *29*, 1345.
(14) Needham, D.; McIntosh, T. J.; Lasic, D. D. *Biochim. Biophys. Acta, Biomembr.* **1992**, *1108*, 40.
(15) Delgado, C.; Francis, G. E.; Fisher., D. *Crit. Rev. Ther. Drug* **1991**, *9*, 249.
(16) Bedu-Addo, F. K.; Huang., L. *Adv. Drug. Delivery Rev.* **1995**, *16*, 235.
(17) Owens Iii, D. E.; Peppas, N. A. *Int. J. Pharm.* **2006**, *307*, 93−102.